Desalination and Water Treatment
www.deswater.com

doi:10.5004/dwt.2017.20412

72 (2017) 1–12
April

Effect of initial feed and draw flowrates on performance of an 8040 spiral-wound forward osmosis membrane element

Seungho Kook[a], Jungeun Kim[b], Sung-Jo Kim[a], Jinwoo Lee[a], Doseon Han[a], Sherub Phuntsho[b], Wang-Geun Shim[b], Moonhyun Hwang[c], Ho Kyong Shon[b], In S. Kim[a,c,*]

[a]*School of Earth Sciences and Environmental Engineering, Gwangju Institute of Science and Technology (GIST), 123 Cheomdangwagi-ro, Buk-gu, Gwangju 61005, Korea*
[b]*Centre for Technology in Water and Wastewater, School of Civil and Environmental Engineering, University of Technology Sydney (UTS), P.O. Box 123, 15 Broadway, NSW2007, Australia*
[c]*Global Desalination Research Center, Gwangju Institute of Science and Technology (GIST), 123 Cheomdangwagi-ro, Buk-gu, Gwangju 61005, Korea, email: iskim@gist.ac.kr (I.S. Kim)*

Received 9 September 2016; Accepted 1 December 2016

ABSTRACT

This study investigated the effects of initial feed (20–50 L/min) and draw flowrates (2–5 L/min) on 8040 spiral-wound FO element performances in serial configuration for a forward osmosis and reverse osmosis (FO-RO) hybrid system employing single element-based tests. Average $J_{w,ave}$ values for varying feed and draw flowrates were found to be 20.93, 19.38 and 18.71 LMH at E1, E2 and E3 (first, second and third elements in a serial configuration), respectively, with averaged diluted draw concentrations of 12.55, 7.88 and 5.77 g/L (initial conc. = 35 g/L). The draw stream dilution was not governed by $J_{w,ave}$ but by the initial draw flowrates at the inlet that governs the retention time of the draw water body in the element. To sum up the performance results, it was concluded that initial draw flowrate is found to govern the performances of FO elements in series in terms of both production of diluted draw stream, determined by the averaged water flux of the FO element, $J_{w,ave}$, and the degree of draw stream dilution. Specific energy consumptions (SECs) of RO were estimated with varying RO feed concentrations (i.e. diluted draw concentration); it was observed the efficiency of SEC reduction by the dilution significantly decays after a critical RO recovery rate. This study successfully provides a valuable insight for feasible application of the FO-RO hybrid system.

Keywords: Forward osmosis; Spiral-wound FO; Flowrate; Draw solution; Energy consumption

1. Introduction

Forward osmosis (FO) process has been suggested as a novel desalination technology to replace existing seawater reverse osmosis (SWRO) process for the last decade [1–3]. In a recent work, however, a critical thermodynamic assessment on FO as a stand-alone desalination process was conducted and reported that FO cannot be an independent process due to the nature of draw solution which has higher osmotic pressure than the seawater. This requires additional energy to treat the diluted draw solution which exhibit higher osmotic pressure than seawater even after the dilution by FO [3]. Although, there are two known examples of stand-alone FO plants (i.e. Al Khaluf (100 m^3/d) and Al Najdah (200 m^3/d) using seawater as feed and evaporative cooling agent as draw solution) in Oman constructed by Modern Water [4,5], the implementation of the stand-alone FO process still has uncertainties and its applicability is not clearly proven that the process is economically feasible. After the dilution of cooling agent in the FO step, the diluted draw stream is guided to the following evaporative regeneration step. It was argued that the Al Kahluf FO plant was operated at 4.9 kWh/m^3 of specific energy consumption (SEC) and showed less energy consumption than

*Corresponding author.

8.5 kWh/m^3 of SEC for reverse osmosis (RO) plant (The Public Authority for Electricity and Water (PAEW) Site at Al Khaluf, 100 m^3/d) [5] but this argument is still invalid because the energy required to regenerate the osmotic agent is not considered and energy recovery devices (ERDs) were not taken into account in assessing the SEC for its relatively smaller total capacity of 100 m^3/d compared to conventional SWRO plants in large scale. It was known that, if the total capacity of the SWRO plants is in large scale, the SEC can reach even below 4.0 kWh/m^3 by considering ERDs [6]. In this respect, there still are practical hurdles in materializing the stand-alone FO desalination plant.

The FO-RO hybrid process has been suggested to reduce the energy consumption in desalination plants [7]. Here, FO functions as a pretreatment followed by RO in this scheme by diluting the seawater with impaired water sources and transporting the diluted seawater to the following RO process to lower the energy consumption and improve the overall plant cost effectiveness. There are studies proposing potential economic benefits of the FO-RO hybrid system over conventional SWRO [8,9] but with ambiguous assumptions on employing FO membrane elements with performances by employing either assuming water flux at 10 LMH or multiplying conversion factors based on lab-scale experiments that are not clearly proven in element-based tests. In particular, one of the key factors that contribute to the economic aspect is the amounts of intake for both impaired water source and seawater. The intake amount initially leads to the determination of input flowrates for the FO process and its specifications of pretreatments before the FO step. The intake thus systematically functions as the guideline for determining pump capacity and the number of pumps required for both feed and draw streams of the FO process. Thus, it is necessary to offer fundamental guidelines for to support a reliable and practically valid economic feasibility analysis based on actual element-based performance. There are studies which estimated the FO element performances [10–12] and actually presented performances with [13–16] and without [17] computational simulation techniques, yet, at smaller dimensions (i.e. 2521, 2540 and 4040; the first two digits represent the element diameter in inch, namely 4.0 inch not 40 inch. The last two digits specify the element length in inch, namely 40 inch not 4.0 inch. In short, a 4040 spiral-wound element has a diameter of 4.0 inch and a length of 40 inch) than 8040, not suitable for economic assessment. Nevertheless, there are studies that reported the performances of 8040 FO elements for fertilizer drawn forward osmosis (FDFO) for direct fertigation using brackish water as feed at single element-based scheme, but validation of FO membrane element performances in serial configuration has not been targeted [18,19].

The major driving force for FO is the osmotic pressure difference between the feed and draw streams and it is necessary to stress the fundamental aspect of FO; the draw stream plays a critical role in generating the osmotic pressure difference within the elements and consequently draw water from the feed streams. Thus, it can be hypothesized that the initial draw flowrates will govern membrane element performances (i.e. water fluxes of elements in series, production of diluted draw streams and dilution of initial draw streams in correlation with retention time) while initial feed flowrates have negligible impacts; a higher initial draw flowrate is expected to yield a higher averaged water flux of an FO membrane element due to a faster replenishment of osmotic driving force and a lower degree of dilution of draw streams due to lower retention time of the draw water body in the membrane element. In the previous work, the impact of feed (i.e. 10–26 L/min) and draw flowrates (i.e. 2–12 L/min with circulating draw stream) on element performance was analyzed using a 4040 FO element but not targeting the performance of FO elements in series [14]. In another study, two cellulose triacetate (CTA) 8040 FO elements from Hydration Technology Innovations (Albany, OR, USA) were tested at feed flowrates of 50, 70 and 100 L/min and a fixed draw flowrate of 0.5 L/min but with circulating draw stream [18]. In a most recent work, 2521 HTICTA FO elements were tested as the two identical elements in parallel and serial configurations at feed and draw flowrates of 3.3–6.6 L/min and 0.35–0.55 L/min, respectively, also with circulating draw streams [17].

In a practical perspective, connecting the FO elements in series is of critical importance to achieve desired RO feed concentration in the FO-RO hybrid system since the energy cost reduction is primarily induced by the seawater dilution in the FO step. Employing spiral-wound FO membrane elements can be advantageous in the hybrid process with RO due to the use of pressure vessels with similar dimensions and shapes leading to the compatibility of the FO process in the perspective of operating and maintenance (O&M). Also, the maximum number of FO elements to be installed in a pressure vessel is one of the governing factors that contribute to the total CAPEX of the FO-RO hybrid system. Thus, it is important to suggest a guideline to limit the maximum number of FO elements in series in a pressure vessel for the FO-RO hybrid system to be optimized based on the actual operational data considering the reduction in RO energy consumption due to dilution of seawater.

The objective of this study is to perform single element-based tests to mimic a serial configuration of up to three 8040 FO membrane elements considering initial feed and draw flowrates as major independent variables without circulating draw streams to maintain osmotic driving force with time. The resulting water flux patterns and degrees of dilution of draw solution were systematically analyzed as the element number increases in series and a feasible approach to determine the maximum element number was suggested. This is the first study that suggests the 8-inch FO membrane element performances in serial configuration utilizing the single element-based tests.

2. Materials and methods

2.1. Single module FO pilot testing system

Fig. 1 illustrates the single module FO pilot testing system utilized for this study. The FO membrane module consists of an FO membrane element and a pressure vessel that can withstand an operating pressure of up to 30 bar. To minimize the effect of hydraulic pressure within the element on the membrane performance, the pressure difference (ΔP) between the feed outlet and the draw inlet was maintained at 0.21 ± 0.01 bar; the pressure difference ensures stable and safe FO operation that such minor pressure on the feed side prevents membrane leaves from rupturing of the glue lines (i.e. membrane

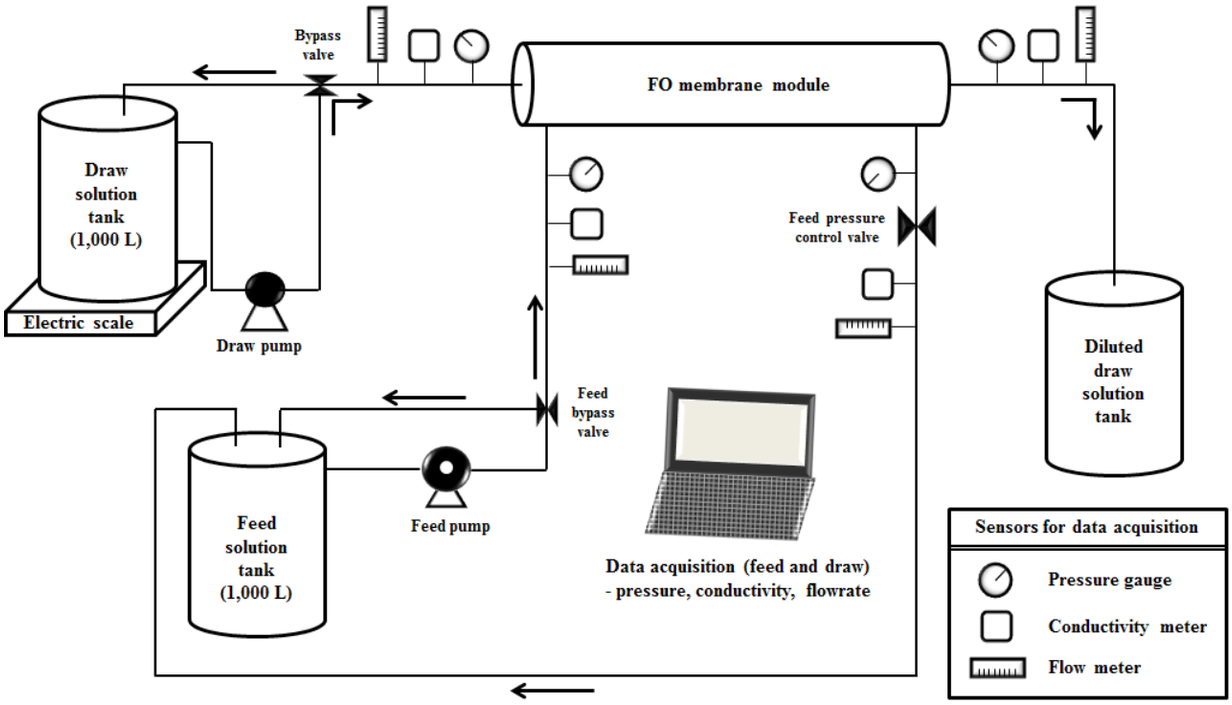

Fig. 1. Schematic of the single module FO pilot testing system.

failure due to rupturing). The desired ΔP was maintained by adjusting the bypass and pressure control valves.

The 8-inch FO membrane element employed for this study was a spiral-wound CSM RE8040-FO. The element contains 10 polyamide thin-film composite (PA-TFC) membrane leaves with total effective membrane area of 15 m^2. The feed stream was circulated and the feed solutions for the following elements were produced with concentrations that matched to the concentrations at the feed outlet of the previous elements. On the contrary, the draw streams were not circulated and the diluted draw streams were collected and employed as the input draw streams for the following elements. Average water flux ($J_{w,ave}$, L/m^2/h or LMH) of the element was computed by incorporating effective membrane area and the flowrates at the inlet and outlet of the draw channel; the flowrates were automatically recorded every minute. The $J_{w,ave}$ values for each test remained consistent due to the non-circulating draw streams. The flowrate data of initial 30 min were utilized to ensure rational comparison of the $J_{w,ave}$ values due to depletion of draw solutions. Eq. (1) shows the $J_{w,ave}$ calculation.

$$J_{w,ave} = \frac{Q_{D,out} - Q_{D,in}}{A_{eff}} \times 60 \quad (1)$$

where $Q_{D,out}$ is the draw flowrate (L/min) at the outlet, $Q_{D,in}$ is the draw flowrate (L/min) at the inlet and A_{eff} is the effective membrane area (m^2) of the membrane element and the equation is multiplied by 60 for time conversion. The calculated $J_{w,ave}$ values were compared with the $J_{w,ave}$ calculated using the weight change of the draw solution tank and ensured that the flux variations were identical. Conductivity (μS/cm for feed and mS/cm for draw) and pressure (bar) values were automatically collected at the inlets and outlets of both feed and draw sides. The conductivities were converted to concentrations (g/L) using a conductivity-concentration standard curves. To compute average reverse solute flux ($J_{s,ave}$, mol/m^2/h), the feed conductivity data of initial 10 min of operations were employed to minimize the effect of circulating feed streams. The resulting $J_{w,ave}$ and $J_{s,ave}$ values gave the characteristic reverse solute diffusion ($J_{sw,ave}$ = $J_{s,ave}/J_{w,ave}$, mol/L) of each element-based test.

2.2. Single element-based serial configuration FO testing

Fig. 2 depicts the single element-based serial configuration testing procedure. Q is the flowrate (L/min) and C is the concentration (g/L). The subscripts F and D represent the feed and draw streams, respectively. E1, E2 and E3 represent the element number in the serial configuration. All tests were carried out in the co-current manner (i.e. feed and draw inlet streams transported into the element from the same side) and the numbers in the subscripts indicate the numerical order of the tests to mimic the serial configuration of the FO membrane elements. This study employed single element-based batch operation and the system was rinsed with tap water after each run. The volume of initial feed solution was 1,000 L and recreated prior to each run by matching the concentration at the feed outlet of previous experiments (e.g. E1 or E2). Also, the initial volume of draw solution was 1,000 L and collected after dilution using a separate tank with identical volume. Operation was conducted until the collected diluted draw solution completely filled up the diluted draw solution tank as depicted

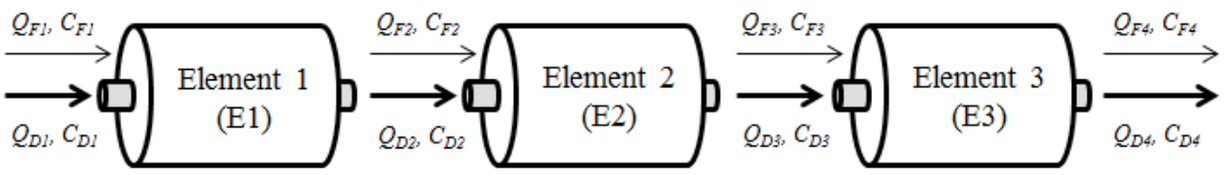

Fig. 2. Illustration of the single element-based serial configuration test procedure.

Table 1
Operating conditions for the single element-based serial configuration FO tests

Operational factors	Description	Note
Membrane element	CSM RE8040-FO	Woongjin Chemical (at present, Toray Chemical)
Effective membrane area (m^2)	15.3	
Initial solutions		
Feed	Tap water (1,000 L)	88.5 ± 3.4 ppm
Draw	35 g/L (1,000 L)	RAM Dried Fine No.2 Salt (99.4% NaCl)
Flowrates (L/min)		
Feed	20, 30, 40, 50	
Draw	2, 3, 4, 5	
Pressure difference, ΔP (bar)	0.21 ± 0.1	ΔP = feed outlet pressure – draw inlet pressure
Temperature (°C)	21.7 ± 0.3	

in Fig. 1. The original draw solution tank was emptied, and cleaned with tap water and refill the tank with diluted draw solution using a separate circulation pump.

Initial feed flowrates (i.e. Q_{F1}) were ranging from 20 to 50 L/min and initial draw flowrates (i.e. Q_{D1}) were 2–5 L/min. To quantify the amount of water drawn by the draw streams, water retrieval rate (Q_R, L/min) was calculated by Eq. (2). The subscript N represents the element number. Q_R can be particularly useful when comparing the data regardless of the amount of initial draw stream input; thus it enables a fair comparison as far as water retrieval is concerned. After all single element-based tests, dilution ratio, DR, was obtained using Eq. (3) to see the degree of dilution compared to the initial draw solution concentration (i.e. seawater concentration = 35 g/L).

$$Q_R = Q_{D,N+1} - Q_{D,1} \left(N = 1,2,3\right) \tag{2}$$

$$R(\%) = \left(1 - \frac{Diluted\ Draw\ Conc.}{Seawater\ Conc.}\right) \times 100 \tag{3}$$

Initial feed solution was 1,000 L of tap water and initial draw solution was 1,000 L of 35 g/L NaCl (99.4% purity, RAM Dried Fine No. 2 Salt, Cheetham Salt, Melbourne, Australia) solution. All tests were conducted at temperature of 21.7°C ± 0.3°C. The operating conditions were summarized in Table 1.

In the FO operation in FO mode (i.e. active layer facing feed solution), the concentrative CP occurs in the vicinity of active layer. However, the impact of concentrative CP in the active layer side was found to have comparably less impacts on determining the membrane performance in the previous study [20], especially when low concentration of feed solution was employed such as the current case. Instead, the internal CP occurrence in the support layer has a critical impact on the membrane performance.

2.3. Effect of draw stream dilution on SWRO SEC in the FO-RO hybrid system

Potential impact of the dilution of draw streams in serial configuration on SWRO SEC was estimated based on the input concentration. ROSA9 software (DOW Water & Process Solutions, USA) was used to simulate the SEC of conventional 2-stage SWRO process with a final product rate of 100,000 m^3/d. Target RO recoveries varied from 40% to 80% in the simulation. SW30XLE-440i element (DOW FILMTEC, USA) was selected as a model SWRO element with varying input concentrations from 5,000 to 35,000 mg/L NaCl to mimic a wide range of concentrations of the diluted draw streams transported from the FO process. As the final outcome, an optimal SEC curve that connects the lowest SECs for respective input RO concentration was generated to find the critical RO feed concentration at which the effect of dilution on the SEC reduction starts to diminish. Energy recovery devices (ERDs) were not incorporated in the simulation.

3. Results and discussion

3.1. Effect of initial feed and draw flowrates on flux variations

3.1.1. Average water flux ($J_{w,ave}$) variations

Fig. 3 shows the $J_{w,ave}$ variations with initial feed and draw flowrates as independent variables. $J_{w,ave}$ of E1 shows the highest water flux regardless of initial flowrates. As the

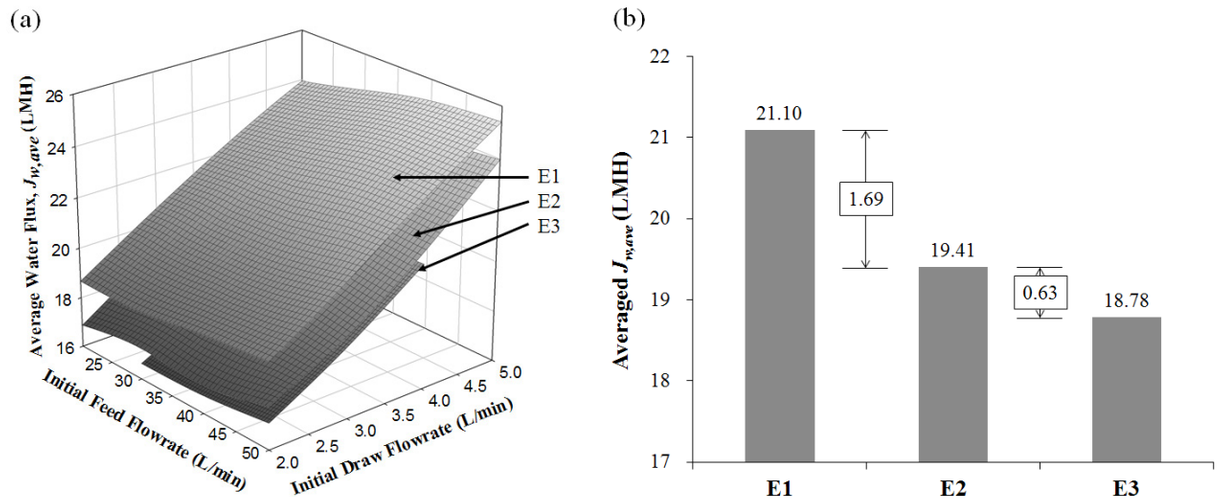

Fig. 3. (a) $J_{w,ave}$ variations with respect to initial feed and draw flowrates, and (b) averaged $J_{w,ave}$ values for E1, E2 and E3 (Note for (b): data utilized from initial feed flowrates of 30–50 L/min and initial draw flowrates of 2–4 L/min).

element number increases (i.e. as the draw streams kept traveling through the draw channels), $J_{w,ave}$ decreased due to the loss of osmotic driving force. The $J_{w,ave}$ values of E1, E2 and E3 were in the ranges of 18.7–25.4 LMH, 16.9–24.0 LMH and 16.6–21.0 LMH, respectively. The non-circulating draw stream enables the system to yield consistent $J_{w,ave}$ values with maximum standard deviation of ±0.12 LMH throughout the operation time regardless of operating conditions. For appropriate comparison, data points of initial 30 min were utilized to minimize the effects of concentrating feed stream due to feed stream circulation and the water level changes in the feed and draw tanks.

Analyzing the slopes of the plots in Fig. 4(a) and (b), the initial feed flowrates had negligible impacts on the $J_{w,ave}$ whereas the increasing initial draw flowrates significantly affected the $J_{w,ave}$ in a positively correlating manner. Similar trend was observed in a previous study using a 4040 FO element [14]. It can be postulated that the lower the initial draw flowrates (i.e. lower draw stream cross flow velocity), the higher the retention time of the draw water body until it exits the elements. Despite the higher retention time of the draw streams at lower initial flowrate, the $J_{w,ave}$ was lower. According to [10], the degree of external concentration polarization (ECP) was simulated under varying cross flow velocities ranging from 0.001 to 1 m/s; it was concluded that lower draw cross flow velocity resulted in a severer ECP reducing the effective osmotic pressure, thus reducing the water flux. The results of this study confirm the previous estimation and suggest that the cause of such low water flux at lower initial draw flowrate can be the severer ECP at lower cross flow velocity.

3.1.2. Variations of reverse solute flux ($J_{s,ave}$) and reverse solute diffusion ($J_{sw,ave}$)

Reverse solute flux is one of the dependent variables for evaluating the performance of FO process. In theory, the water and solute permeations across the FO membrane are collocated in the form of diffusive transports based on the Fick's law and the Henry's law (i.e. no interactions among the species). Assuming the transports of dilute species, Van't Hoff equation can be employed to explain the proportionality of the water and solute transports. Detailed explanation on the theory is given elsewhere [21]. Therefore, the reverse solute flux is relatively proportional to the permeate water flux and the results are given in Fig. 5a. The trend of $J_{s,ave}$ is in sync with the trend of $J_{w,ave}$ depicted in Fig. 3b; this leads to the characteristic solute transport represented as the reverse solute diffusion [22]. $J_{sw,ave}$ remained consistent regardless of the element number as illustrated in Fig. 5b and found within the range of $4.9 \times 10^{-3} \pm 0.6 \times 10^{-3}$ mol/L for all operating conditions following the theory.

For better visualization, Fig. 6 shows the $J_{s,ave}$ results for a set of operating conditions (i.e. fixed feed flowrate of 40 L/min and fixed draw flowrate of 4 L/min) that can represent the operating conditions of this study. As discussed, for the fixed feed flowrate, the $J_{s,ave}$ variations (Fig. 6a) are in sync with the patterns of $J_{w,ave}$ (Fig. 4a). However, for a fixed draw flowrate, the two relevant figures (i.e. Figs. 4b and 6b) are seemingly not in correlation. For the conventional S-D model, the feed and draw streams in FO operations are assumed to be in the laminar flow region; the initial feed flowrates were approximately 10 times higher than the initial draw flowrates and the severe turbulent flow in the feed channel could induce such trend. The averaged $J_{s,ave}$ for E2 in Fig. 5a is slightly off the trend due to the effect of such turbulent flows in the feed channel. Also, the relatively smaller slopes in Fig. 4b compared to those of Fig. 4a indicates that the calculation of $J_{sw,ave}$ can be within the error range due to the unknown yet minor variables for the element-based FO operations. Though the overall trend of $J_{sw,ave}$ in Fig. 5b follows the general concept of the theory.

3.2. Impact of initial flowrates on the water retrieval by draw streams

Along with water flux and reverse solute flux, volumetric production of diluted draw stream and the degree of

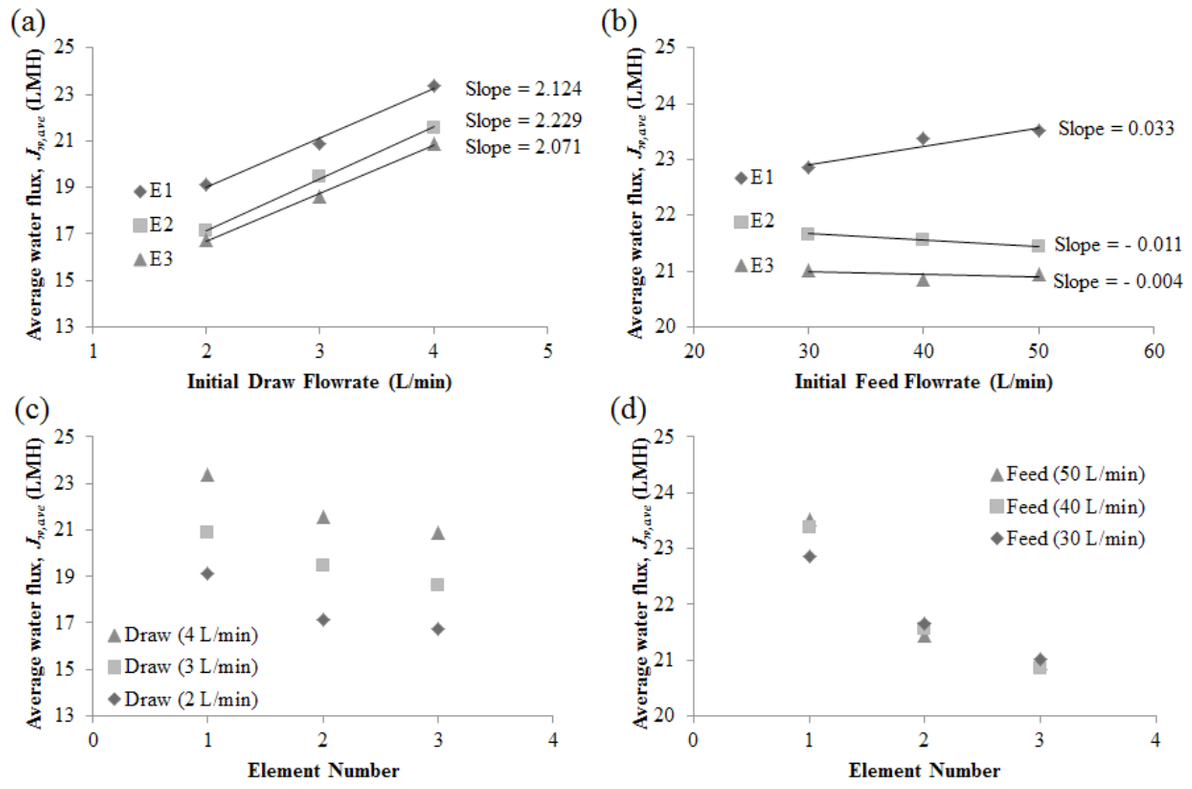

Fig. 4. $J_{w,ave}$ variations with (a) varying initial draw flowrates at the fixed initial feed flowrate of 40 L/min, (b) varying initial feed flowrates at the fixed initial draw flowrate of 4 L/min, (c) the increasing element number at the fixed initial feed flowrate of 40 L/min, and (d) the increasing element number at the fixed initial draw flowrate of 4 L/min.

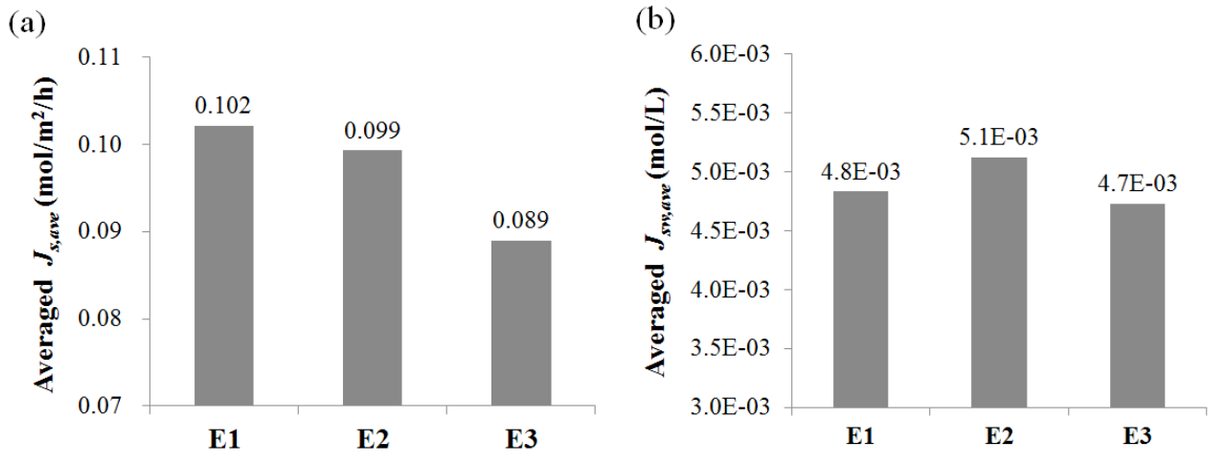

Fig. 5. Variations of (a) averaged $J_{s,ave}$ and (b) averaged $J_{sw,ave}$ depending on the element number (Note: data utilized from initial feed flowrates of 30–50 L/min and initial draw flowrates of 2–4 L/min).

dilution are of their critical importance due to the field-oriented nature of element-based operations since the two parameters function as the major design factors for the following RO process in the FO-RO hybrid scheme. Here, water retrieval rates of each element were computed to offer basis for determining the maximum FO membrane element in an FO pressure vessel.

As observed in Figs. 3 and 4, the initial feed flowrates have negligible impacts on $J_{w,ave}$. Initially, $J_{w,ave}$ and Q_R were computed based on the draw flowrates at the inlet and outlet [i.e.

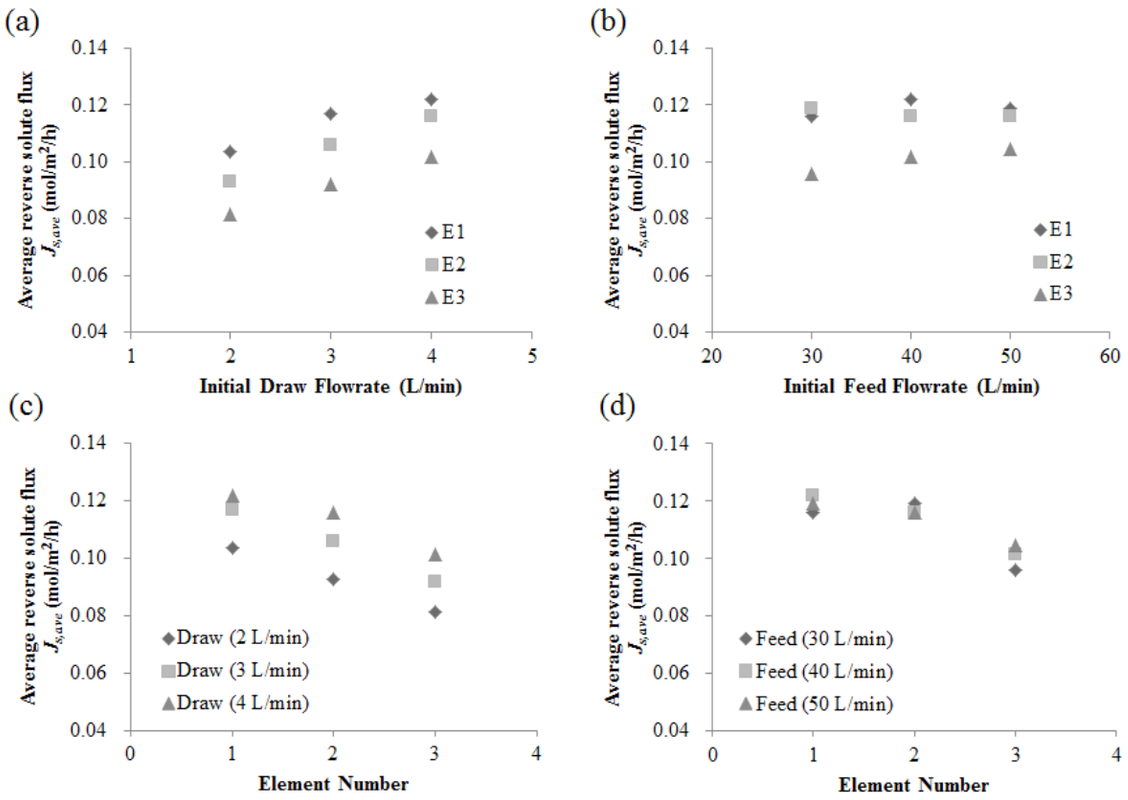

Fig. 6. $J_{s,ave}$ variations with (a) varying initial draw flowrates at the fixed initial feed flowrate of 40 L/min, (b) varying initial feed flowrates at the fixed initial draw flowrate of 4 L/min, (c) the increasing element number at the fixed initial feed flowrate of 40 L/min, and (d) the increasing element number at the fixed initial draw flowrate of 4 L/min.

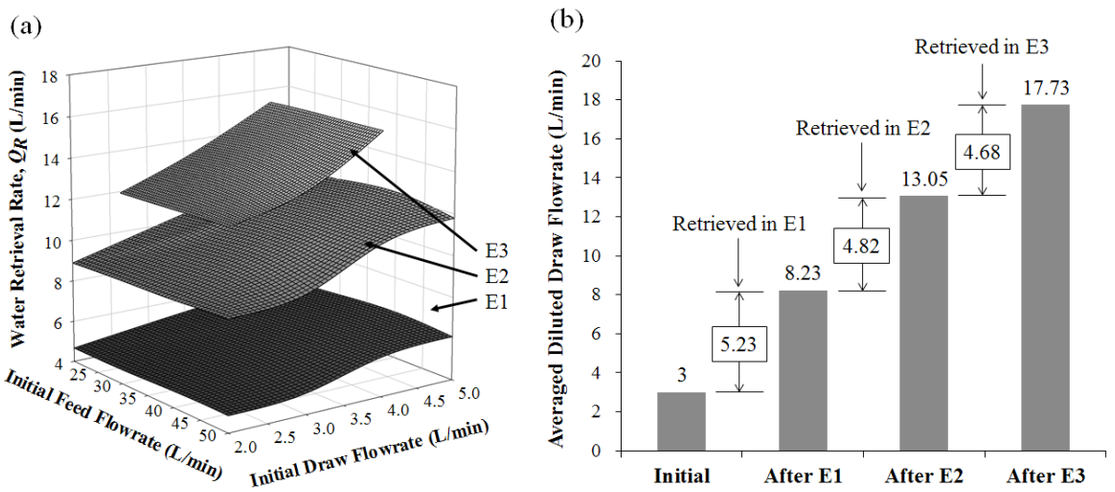

Fig. 7. (a) Impact of initial feed and draw flowrates on water retrieval rates, Q_R, and (b) averaged diluted draw flowrates after E1, E2 and E3 (Note for (b): data utilized from initial feed flowrates of 30–50 L/min and initial draw flowrates of 2–4 L/min (average: 3 L/min)).

Eqs. (1) and (2)] and thus the nature of the two dependent variables is equal. It can be expected that the initial feed flowrates have also a negligible impact on the production of diluted draw streams. The identical logic applies to the initial draw flowrates and their impacts are expected to be noticeable. Fig. 7 depicts the effects of the initial feed and draw flowrates on the water retrieval rates, Q_R, of FO elements assumed to be in series. Q_R increased as the element number increased; the Q_R values for E1, E2 and E3 were observed to be within 4.7–11.3 L/min, 8.9–17.2 L/min and 15.1–20.5 L/min, respectively.

Fig. 8 shows Q_R variations for the representative set of operating conditions with respect to changing initial feed and draw flowrates and the patterns between the FO elements. Fig. 8b and 8d clearly show the initial assumption on the feed flowrates that, for a fixed initial draw flowrate, the initial feed flowrates indeed have negligible impact on the water transport toward the draw streams. On the other hand, Q_R was significantly deviated with an apparent increasing pattern as both the initial draw flowrates and the increasing element number (Fig. 8a and 8c). Initial draw flowrate and the water retrieval rate of each element together directly influence the dilution of draw streams. Further discussion is made by co-locating Q_R with the dilution of draw streams in the following section.

3.3. Effect initial feed and draw flowrates on the dilution of draw streams

With the increasing number of FO membrane elements in series, the degree of dilution increases. Fig. 9 depicts the pattern of diluted draw solution concentrations exiting the three elements (i.e. E1, E2 and E3) consecutively. After E1, the resulting draw solution concentration varied within 10.4–15.8 g/L (i.e. *DR*: 70.4–54.8%). The diluted draw stream concentrations after E2 and E3 were in the ranges of 6.3–10.4 g/L (i.e. *DR*: 82.0%–70.2%) and 4.5–6.9 g/L (i.e. *DR*: 87.0%–80.2% dilution), respectively. The concentrations of diluted draw streams maintained consistency with maximum standard deviation of ±0.22 g/L for all operating conditions with the help of the non-circulating draw streams.

The increments in *DR* decreased significantly as the element number increased due to the loss of osmotic gradient as the initial draw stream experiences the consecutive dilution by FO elements in series. A noticeable dilution of draw stream was observed at E1 (Fig. 9b), suggesting that the first element out of a group of FO elements in series plays a pivotal role for dilution.

As noted, at a fixed initial draw flowrate, initial feed flowrates do not significantly affect the dilution of draw streams, which shows the similar pattern with the impact of feed streams on the $J_{w,ave}$. The initial draw flowrates, on the other hand, have a significant effect on the dilution of the draw streams. It is important to note that the diluted draw solution concentration (Fig. 10a) has positive correlation with the pattern of $J_{w,ave}$ (Fig. 4a), the intriguing pattern that clearly indicates the higher water flux yielding lower degree of dilution. Higher diluted draw solution concentration and higher $J_{w,ave}$ at higher initial draw flowrate (i.e. shorter retention time of the draw streams) confirms the hypothesis that the higher initial draw flowrate reduces the draw stream dilution. These results address an important finding that, for spiral-wound FO membrane elements, higher $J_{w,ave}$ does not necessarily lead to better dilution of the draw streams, which have never been discussed in the pilot-scale tests [14,17,18].

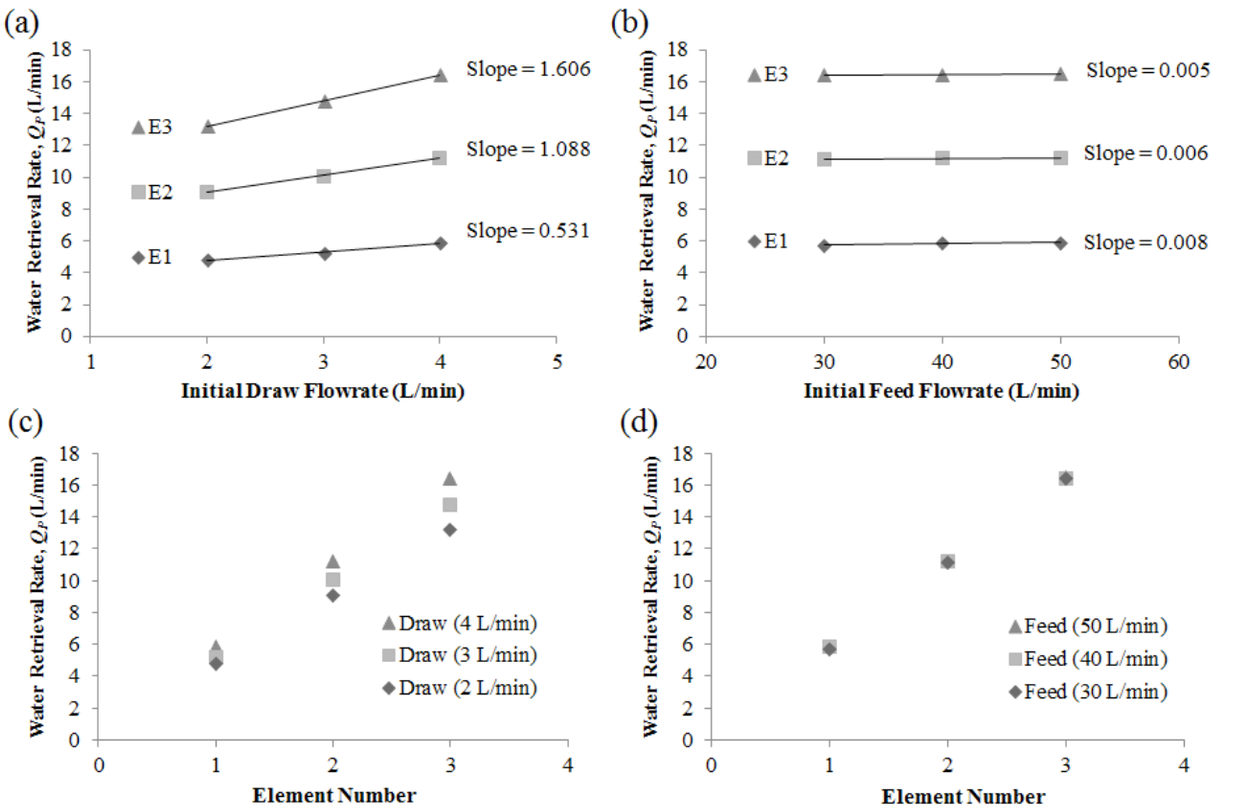

Fig. 8. Q_R variations with (a) varying initial draw flowrates at the fixed initial feed flowrate of 40 L/min, (b) varying initial feed flowrates at the fixed initial draw flowrate of 4 L/min, (c) the increasing element number at the fixed initial feed flowrate of 40 L/min, and (d) the increasing element number at the fixed initial draw flowrate of 4 L/min.

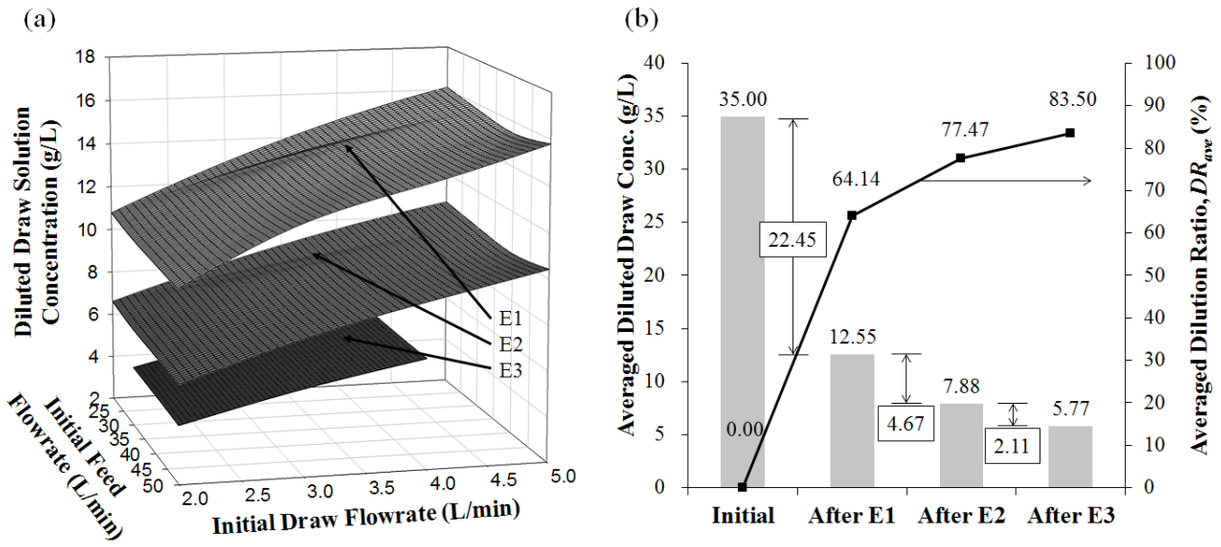

Fig. 9. (a) Diluted draw solution concentrations exiting the membrane elements in series, and (b) averaged diluted draw solution concentrations and dilution ratio for E1, E2 and E3 (Note for (b): data utilized from initial feed flowrates of 30–50 L/min and initial draw flowrates of 2–4 L/min).

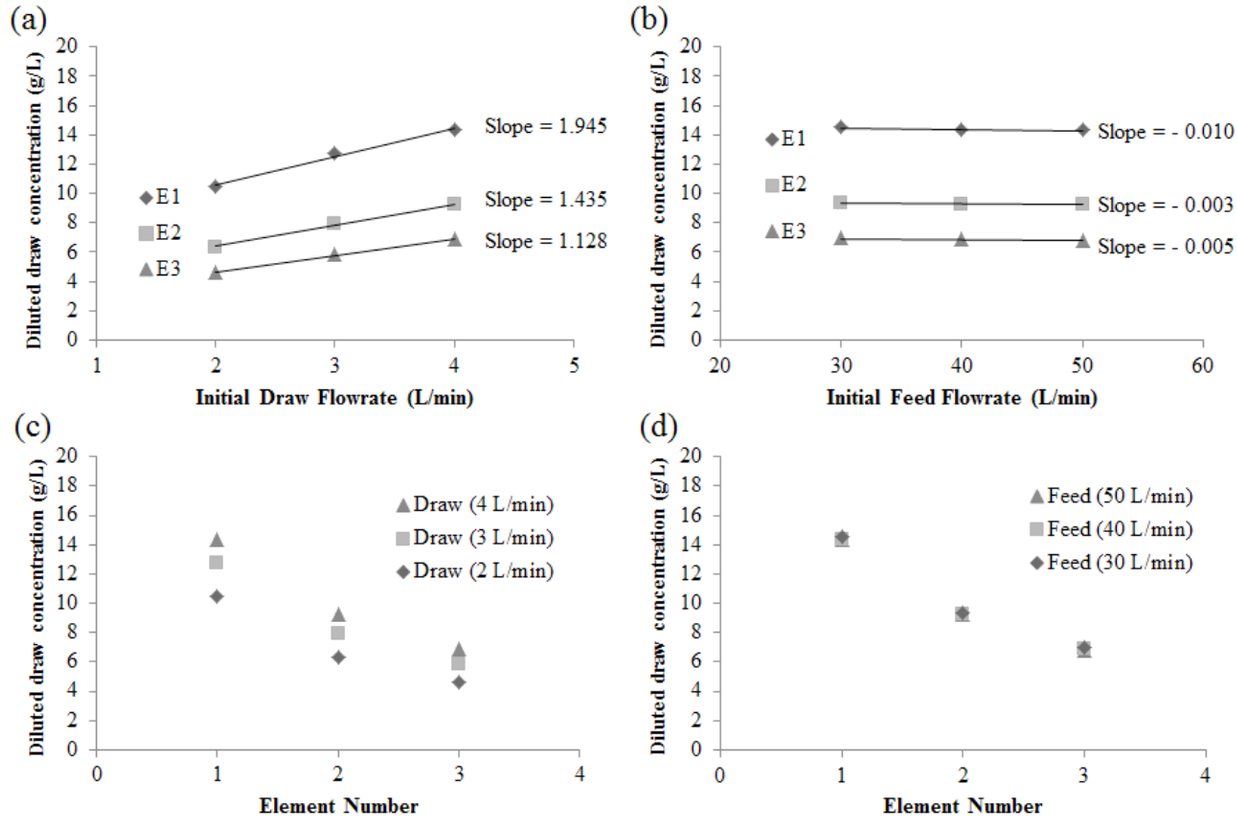

Fig. 10. Diluted draw solution concentration variations with (a) varying initial draw flowrates at the fixed initial feed flowrate of 40 L/min, (b) varying initial feed flowrates at the fixed initial draw flowrate of 4 L/min, (c) the increasing element number at the fixed initial feed flowrate of 40 L/min, and (d) the increasing element number at the fixed initial draw flowrate of 4.

In the three previous works, the diluted draw streams were recirculated back to the draw solution tank. However, imposing a constant osmotic driving force by not circulating the draw stream, the operating condition employed in this study, was able to distinguish the effect of dilution by FO from that induced by recirculation.

This trend spotlights the ratio between water permeation velocity (i.e. represented as $J_{w,ave}$) and draw stream velocity. $J_{w,ave}$ of 20 LMH is equivalent to the water permeation velocity of 5.56×10^{-6} m/s and, assuming a membrane leaf inlet cross section of 0.4 m × 0.002 m, 4 L/min of initial draw flowrate (i.e. 0.4 L/min for one membrane leaf) can be calculated as 8.33×10^{-3} m/s; let this case represent the data presented above since the $J_{w,ave}$ values in Fig. 3 varied within 20 ± 4 LMH. The draw stream velocity is approximately 1,498 times bigger as opposed to the water permeation velocity. This indicates the water permeation velocity (i.e. $J_{w,ave}$) has negligible impact on draw stream dilution due to the significantly lower contact time of the permeate water at a specific location within an element with the draw water body traveling at extremely higher velocity as specified above. In short, the traveling draw water body collects the permeate water from different locations as it passes through the draw channel. Though, the $J_{w,ave}$ could be a major factor for dilution only when the draw stream velocity becomes comparable to the water permeation velocity.

Nevertheless, the dilution of draw stream cannot be defined without $J_{w,ave}$ since water flux is the only source for the dilution in the form of water retrieval in each element. Therefore, $J_{w,ave}$ affects the draw stream dilution yet to a significantly small extent. In this respect, by collocating the patterns of $J_{w,ave}$ and diluted draw solution concentration, it can be concluded that the retention time of the initial draw water body governs the draw stream dilution as the major factor while $J_{w,ave}$ takes part in as a minor one.

Fig. 11 summarizes how the initial feed and draw flowrates in an FO serial configuration determines the production of the RO feed streams. The initial feed flowrate is a minor factor in altering element performances analyzing the results in Fig. 4b and 4d and Fig. 8b and 8d yet it still participates as an active one for its presence in collaboration with the draw stream for generating $J_{w,ave}$. Initial draw flowrate actively engages in generating $J_{w,ave}$ by offering osmotic gradient across the membrane but, more importantly, it determines the retention time of the draw water body within FO elements. The retention time primarily controls the draw stream dilution and governs the RO feed water quality. $J_{w,ave}$ can be interpreted as water retrieval rate (Q_R) in a practical aspect. Q_R is then be added to initial draw flowrate ($Q_{D,in}$) to yield the RO feed flowrate. By summing up the important findings of this study, it can be drawn that controlling the initial draw flowrate is key in accomplishing the task of FO (i.e. both volumetric production of diluted draw stream and its dilution) in the FO-RO hybrid system.

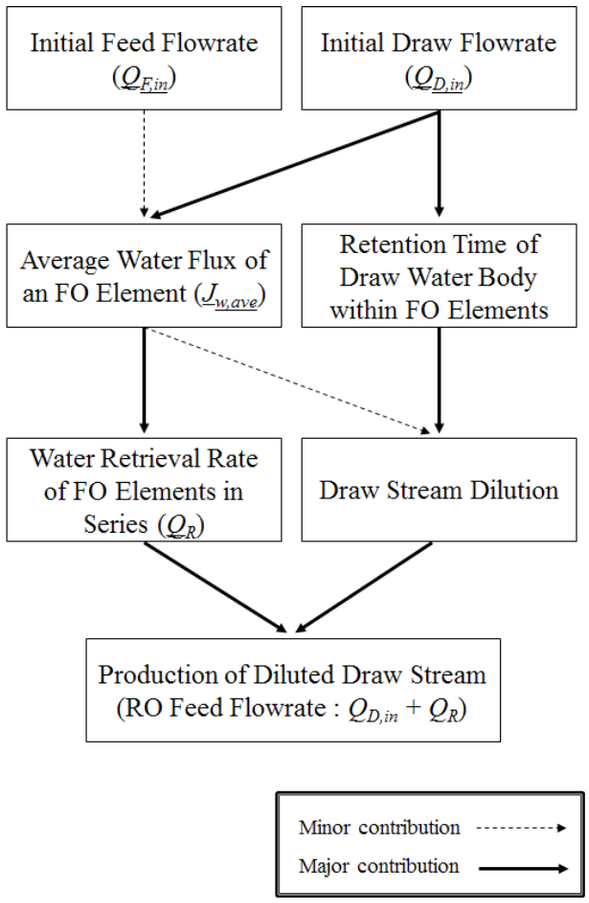

Fig. 11. Flow diagram for production of diluted draw streams (i.e. RO feed streams).

3.4. Effect of draw stream dilution on SWRO SEC in the FO-RO hybrid system

The RO process can produce the same amount of the final product water with less energy consumption in the case when the RO feed stream with lower concentration than the seawater is introduced to RO based on thermodynamics [23], the fundamental aspect and motivation of implementing the FO-RO hybrid system. The ROSA simulation results suggest the estimated SECs for a fixed final product of 100,000 m^3/d and the resulting optimal SECs (i.e. lowest SECs) for varying RO feed concentrations (Fig. 12).

As noted in Fig. 9b, the averaged concentrations of diluted draw streams after E1, E2 and E3 were 12.55, 7.88 and 5.77g/L (i.e. 62.5%, 76.2% and 83.5% dilution), respectively. In Fig. 12a, the SEC_{opt} for 35 g/L (i.e. seawater as RO feed for conventional 2-stage RO) was 3.82 kWh/m^3. For the averaged draw stream concentrations after E1, E2 and E3 in the FO-RO hybrid scheme, the SEC_{opt} values for RO were estimated to be 1.55, 1.11 and 0.88 kWh/m^3 (i.e. 59.5%, 71.0% and 76.9% reduction in RO energy consumption), respectively.

Another key aspect of the FO-RO hybrid is the RO recovery enhancement by seawater dilution which can directly be postulated as the reduction of RO feed intake capacity which contributes to the total cost reduction of the hybrid process. It was found that the SEC_{opt} values were in between 55% and 75% of RO recoveries in a decaying pattern as the RO recovery escalates (Fig. 12b).

As noted, the slope of the SEC_{opt} plot stays consistent up to the RO recovery of approximately 65%, suggesting that RO energy consumption decreases in a linear relation

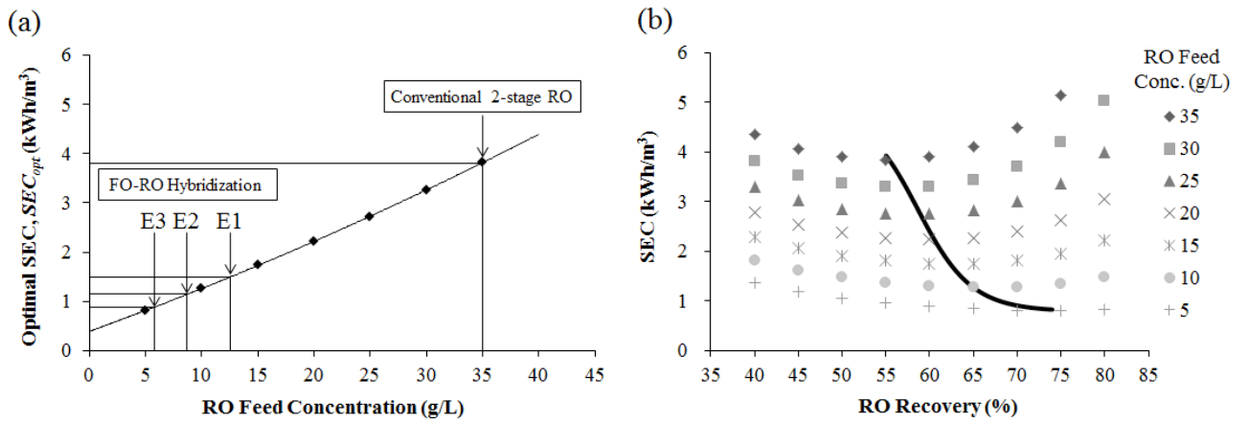

Fig. 12. (a) SEC_{opt} plot with respect to RO feed concentration for 100,000 m^3/d of the final product employing SW30XLE-440i as model SWRO element, and (b) simulated SECs with varying RO recovery and the regression plot (i.e. the black curve) which represents the SEC_{opt} within the range of 5–35 g/L of RO feed concentration.

with RO recovery as the RO feed concentration decreases (i.e. concentration of diluted draw stream); yet it starts to diminish beyond the critical point (i.e. 65% RO recovery). This implies that, in the FO-RO hybrid system, the economic benefit of reducing RO energy consumption induced by diluting seawater starts to decrease significantly above the critical point. At the same time, by properly accounting the pattern of draw stream dilution depicted in Fig. 9b, it can be reasonably estimated that FO CAPEX, more specifically the costs for FO elements, would start to significantly increase beyond the critical point if further dilution of draw stream is demanded. In short, further dilution of the draw stream beyond this critical RO recovery rate would cause only marginal economic benefits compared to conventional 2-stage RO.

Considering the energy aspects of FO-RO hybrid, the estimated maximum number of spiral-wound 8040 FO elements in series for the fixed final RO product (i.e. 100,000 m^3/d) can be 2 for this specific case. Though, the maximum number of FO elements in series can vary depending on the total capacity of the FO-RO hybrid plant and the desired diluted draw stream concentration for the RO process; the estimated number can be altered if other CAPEX and OPEX components of both FO and RO are taken into account in an accurate and thorough economic feasibility assessment. Also, applying small additional pressure on the feed side [22], namely the pressure-assisted forward osmosis (PAFO), can further reduce the maximum element number due to more efficient dilution of the draw stream, thereby reducing the required FO membrane area for target dilution ratio for the RO process. In this respect, current work can serve as the basis for further optimization of the following RO process design for better understanding on the economics of the FO-RO hybrid system.

4. Conclusions

The effects of initial feed and draw flowrates on the performances of FO elements in series were discussed in this study, utilizing a spiral-wound 8040 PA-TFC FO element tomimic a serial configuration of the FO membrane elements up to 3 based on single element-based tests. A series of key findings were drawn:

- It was hypothesized the initial draw flowrate would govern the membrane performances and the $J_{w,ave}$ would be higher due to a faster replenishment of osmotic gradient as the initial draw flowrate increases but with diminishing dilution efficiency. The results successfully validated and proved the hypothesis in terms of phenomenological patterns in the membrane performances.
- The results of current study address an important finding that, for spiral-wound FO membrane elements, higher $J_{w,ave}$ does not necessarily lead to better dilution of the draw streams, rather the draw stream dilution is primarily governed by the initial draw flowrate that determines the retention time of the initial draw water body, which have never been discussed in the pilot-scale tests [14,17,18].
- This study also addressed a strategy to properly incorporate the required number of FO membrane elements in series based on their actual performances for an accurate economic feasibility analysis on the hybrid process; the critical RO recovery point shall not be surpassed to prevent the economic feasibility of the hybrid process from being disadvantageous.
- In short, this study successfully found a basis for practical FO operations by focusing on initial feed and draw flowrate sand gave insights on proper accounting of FO for the FO-RO hybrid system and its economic feasibility.

Acknowledgements

This research was supported by a grant (code 16IFIP-B088091-03) from Industrial Facilities & Infrastructure Research Program funded by Ministry of Land, Infrastructure and Transport of Korean government.

References

[1] T. Cath, A. Childress, M. Elimelech, Forward osmosis: Principles, applications, and recent developments, J. Membr. Sci., 281 (2006) 70–87.

[2] S. Zhao, L. Zou, C.Y. Tang, D. Mulcahy, Recent developments in forward osmosis: opportunities and challenges, J. Membr. Sci., 396 (2012) 1–21.

[3] D.L. Shaffer, J.R. Werber, H. Jaramillo, S. Lin, M. Elimelech, Forward osmosis: where are we now?, Desalination, 356 (2015) 271–284.

[4] P.G. Nicoll, Forward osmosis as a pre-treatment to reverse osmosis, The IDA World Congress on Desalination and Water Reuse, IDAWC/TIAN13-318 (2013).

[5] N.A. Thompson, P.G. Nicoll, Forward osmosis desalination: a commercial reality, The IDA World Congress, IDAWC/PER11-198 (2011).

[6] N. Ghaffour, T.M. Missimer, G.L. Amy, Technical review and evaluation of the economics of water desalination: current and future challenges for better water supply sustainability, Desalination, 309 (2013) 197–207.

[7] T.Y. Cath, N.T. Hancock, C.D. Lundin, C. Hoppe-Jones, J.E. Drewes, A multi-barrier osmotic dilution process for simultaneous desalination and purification of impaired water, J. Membr. Sci., 362 (2010) 417–426.

[8] R. Valladares Linares, Z. Li, V. Yangali-Quintanilla, N. Ghaffour, G. Amy, T. Leiknes, J.S. Vrouwenvelder, Life cycle cost of a hybrid forward osmosis - low pressure reverse osmosis system for seawater desalination and wastewater recovery, Wat. Res., 88 (2016) 225–234.

[9] G. Blandin, A.R.D. Verliefde, C.Y. Tang, P. Le-Clech, Opportunities to reach economic sustainability in forward osmosis–reverse osmosis hybrids for seawater desalination, Desalination, 363 (2015) 26–36.

[10] M.F. Gruber, C.J. Johnson, C.Y. Tang, M.H. Jensen, L. Yde, C. Hélix-Nielsen, Computational fluid dynamics simulations of flow and concentration polarization in forward osmosis membrane systems, J. Membr. Sci., 379 (2011) 488–495.

[11] B. Gu, D.Y. Kim, J.H. Kim, D.R. Yang, Mathematical model of flat sheet membrane modules for FO process: Plate-and-frame module and spiral-wound module, J. Membr. Sci., 379 (2011) 403–415.

[12] A. Sagiv, A. Zhu, P.D. Christofides, Y. Cohen, R. Semiat, Analysis of forward osmosis desalination via two-dimensional FEM model, J. Membr. Sci., 464 (2014) 161–172.

[13] Y. Xu, X. Peng, C.Y. Tang, Q.S. Fu, S. Nie, Effect of draw solution concentration and operating conditions on forward osmosis and pressure retarded osmosis performance in a spiral wound module, J. Membr. Sci., 348 (2010) 298–309.

[14] Y.C. Kim, S.J. Park, Experimental study of a 4040 spiral-wound forward-osmosis membrane module, Environ. Sci. Technol., 45 (2011) 7737–7745.

[15] D. Attarde, M. Jain, K. Chaudhary, S.K. Gupta, Osmotically driven membrane processes by using a spiral wound module — Modeling, experimentation and numerical parameter estimation, Desalination, 361 (2015) 81–94.

[16] D. Attarde, M. Jain, S.K. Gupta, Modeling of a forward osmosis and a pressure-retarded osmosis spiral wound module using the Spiegler-Kedem model and experimental validation, Sep. Purif. Technol., (2016).

[17] S.-J. Im, G.-W. Go, S.-H. Lee, G.-H. Park, A. Jang, Performance evaluation of two-stage spiral wound forward osmosis elements at various operation conditions, Desal. Wat. Treat., 57 (2016) 24583–24594.

[18] J.E. Kim, S. Phuntsho, F. Lotfi, H.K. Shon, Investigation of pilot-scale 8040 FO membrane module under different operating conditions for brackish water desalination, Desal. Wat. Treat., 53 (2014) 2782–2791.

[19] S. Phuntsho, J.E. Kim, M.A.H. Johir, S. Hong, Z. Li, N. Ghaffour, T. Leiknes, H.K. Shon, Fertiliser drawn forward osmosis process: Pilot-scale desalination of mine impaired water for fertigation, J. Membr. Sci., 508 (2016) 22–31.

[20] C. Suh, S. Lee, Modeling reverse draw solute flux in forward osmosis with external concentration polarization in both sides of the draw and feed solution, J. Membr. Sci., 427 (2013) 365–374.

[21] C.Y. Tang, Q. She, W.C.L. Lay, R. Wang, A.G. Fane, Coupled effects of internal concentration polarization and fouling on flux behavior of forward osmosis membranes during humic acid filtration, J. Membr. Sci., 354 (2010) 123–133.

[22] G. Blandin, A.R.D. Verliefde, C.Y. Tang, A.E. Childress, P. Le-Clech, Validation of assisted forward osmosis (AFO) process: impact of hydraulic pressure, J. Membr. Sci., 447 (2013) 1–11.

[23] Y.M.E.-S. K.S. Spiegler, The energetics of desalination processes, Desalination, 134 (2001) 20.